Hindawi
Geofluids
Volume 2021, Article ID 6613252, 8 pages
https://doi.org/10.1155/2021/6613252

Research Article

Simulation Experiment of TSR Promotes Cracking of Coal Generation H_2S

Qigen Deng,[1,2,3] **Yinsheng Du**,[1] **Yanjie Yang**,[1] **and Fajun Zhao**[1,2]

[1]*School of Safety Science and Engineering, Henan Polytechnic University, Jiaozuo 454003, China*
[2]*State Key Laboratory Cultivation Base for Gas Geology and Gas Control (Henan Polytechnic University), Jiaozuo 454003, China*
[3]*Collaborative Innovation Center of Coal Safety Production of Henan Province, Jiaozuo 454003, China*

Correspondence should be addressed to Qigen Deng; dengqigen@hpu.edu.cn

Received 8 October 2020; Revised 3 January 2021; Accepted 28 March 2021; Published 3 May 2021

Academic Editor: Guozhong Hu

Thermochemical sulfate reduction (TSR) is one of the main contributors to the formation of hydrogen sulfide (H_2S) in coal seam strata. Four reaction systems (coal, coal+water, coal+water and $MgSO_4$, and coal+water and $MgSO_4$ and $AlCl_3$) were selected and simulated from 250°C to 600°C with eight temperature steps using a high-temperature and high-pressure reaction device, and the evolution characteristics of the gaseous products of hydrocarbons (methane, $C_{2\text{-}5}$) and nonhydrocarbon gases (CO_2, H_2, and H_2S) were studied. Thermal simulation experiments showed that the TSR led to the reduction of heavy hydrocarbons, and the presence of salts accelerated the evolution of hydrocarbons; SO_4^{2-}, Al^{3+}, and Mg^{2+} had a certain promoting effect on the TSR, which increased the total amount of alkane gas, H_2S, and CO_2 production. Improving the salinity of the reaction system can promote the occurrence of TSR, and water plays a key role in hydrocarbon generation evolution and the TSR.

1. Introduction

Abnormal emission and casualty accidents caused by the enrichment of hydrogen sulfide (H_2S) in coal mines occur frequently domestically and internationally. High-sulfur natural gas reservoirs (volume percentage of H_2S greater than 5%) are widely distributed around the world, and all are closely related to the distribution of sulfate reservoirs. Previous studies have shown that thermochemical sulfate reduction (TSR) is one of the main ways to form hydrogen sulfide in oil and gas reservoirs and coal seam strata [1, 2]. The simulation research of scholars domestically and internationally about the thermochemical reduction reaction are mostly concentrated in the field of oil and natural gas, and a large number of cracking and thermal simulation experiments have been carried out [3–6]. TSR research has been carried out for more than 30 years, involving oil and gas geology, mineralogy, geochemistry, experimental geology, and many other fields, and TSR initiation mechanism, production products, influencing factors, isotope fractionation, reaction mechanism, discriminatory markers, limit temperature, and kinetic characteristics have been studied [7–10]. However, there are still few experimental studies on the simulation of thermochemical reduction of coal and sulfate to produce hydrogen sulfide-containing gas. Based on the previous studies, this study adopts the method of high temperature and high pressure where M_{ad} is the air-dried moisture and A_d is the ash dry and thermal simulation experiments under various media conditions in a closed system. The temperature of hydrocarbon formation under geological conditions is about 70~200°C, and the temperature of hydrogen sulfide formed by TSR is 120~200°C. In order to accelerate the reaction, the study chooses a higher temperature and conducts TSR thermal simulation experiments on coal in order to provide theoretical guidance on the evolution and formation mechanism of hydrogen sulfide gas in coal-series strata.

2. Samples and Experimental Methods

2.1. Experimental Samples. An anthracite fresh coal sample used in this experiment was selected from the no. 15 coal seam in a coal mine of Mountain Fenghuang, southern Qinshui Basin, Shanxi Province, China, where the H_2S is

abnormally enriched, and the parameters of the samples were measured. The industrial analysis, elemental analysis, and sulfur composition are shown in Table 1. After the coal sample was crushed, it was sieved out with the particle size of 80-150 μm in the constant temperature vacuum drying oven at 50°C to make a dry sample of 8000 g as the experimental coal sample, and the sieved sample was divided into 8 portions; each portion of 1000 g was stored in a dry bottle and injected with nitrogen and sealed for use.

M_{ad} is the air-dried moisture, A_d is the dry ash, V_{daf} is the dry ash-free volatile, $S_{t,d}$ is the dry basis total sulfur, $S_{o,d}$ is the dry basis organic sulfur, and $S_{p,d}$ is the dry basis pyretic sulfur. The coal of sample no. 15 is mostly black and powdery, and a small part is massive. It is a semibright briquette with mirrored coal ribbon and silk carbon lens. It has a thin-medium strip structure and occasionally white calcite and dispersed, nodular, and film-shaped pyrite.

2.2. Experimental Method. The experimental device mainly consists of a reactor, control device, degassing device, loading device, and gas collection and analysis device. The system diagram is shown in Figure 1 [11]. The maximum temperature control of the system is 650°C, and the accuracy is ±1°C. The maximum pressure control is 25.0 MPa, and the accuracy is ±0.5 MPa. During the experiment, the quartz tube containing 1000 ± 0.1 g of the experimental samples was successively put into the kettle. After connecting all air circuits and temperature sensors of the equipment and detecting the air tightness of each air circuit, the vacuum degasses the entire system. After degassing, different media were injected into the quartz tube in the reactor from the loading device according to the experimental scheme. Into the quartz tube in the reaction kettle, 300 mL of an ion aqueous solution with a molar concentration of 1.0 mol/L of mineral aqueous solution containing additives was injected. The initial pressure in the kettle is set to 5.0 MPa, and the final pressure of the reaction system is between 12.0 and 20.0 MPa. The reaction is heated at a heating rate of 20°C/h, simulating gaseous products at 8 temperature points of 250°C, 300°C, 350°C, 400°C, 450°C, 500°C, 550°C, and 600°C, and these were analyzed. The heating time for each simulation experiment stage was 24 hours. At the end of each experimental stage, the gaseous products in the reactor were collected using a special sampler for hydrogen sulfide and a Tedlar gas sample bag. Using a gas chromatograph, the gaseous products of hydrocarbon gases (methane, heavy hydrocarbons) and nonhydrocarbon gases (CO_2, H_2, and H_2S) were measured.

3. Experimental Results and Discussion

The coal sample used in this experiment can be regarded as a typical porous medium. Its fine particle size and its connected internal channels allow the gas to flow smoothly through its surface and inside, and it is also a place for heat transfer and physical and chemical reactions. The gaseous product test results of hydrocarbon gas (CH_4, $C_{2\sim5}$) and nonhydrocarbon gas (CO_2, H_2, and H_2S) are shown in Table 2.

Coal is a complex polymer compound with condensed aromatic nuclei derived from lignin as the main body, connected by various bridges and carrying various types of fatty and nonfatty functional groups [12]. The coal pyrolysis process begins with the breaking of the fatty carbon-fatty carbon bond (C_{al}-C_{al}), and at about 500~600°C, the aliphatic carbon-hydrogen bond (Cal-H) is broken. The aromatic carbon=aromatic carbon bond (C_{ar}=C_{ar}) on the aromatic ring is very difficult to break during pyrolysis due to its very stable structure. The oxygen-containing structures and other heterocyclic structures in coal break at 400-700°C. Fat carbon-sulfur bridge bond (Cal-S) fracture temperature is usually lower than that of C_{al}-C_{al}, and C_{al}-S bond cleavage promotes free radical formation. In the early stage of thermal evolution at low temperature, the gas adsorbed in the pores of the coal and the weak bonds in the coal structure are broken, and the gases such as CH_4, CO_2, and N_2 are removed. As the thermal simulation temperature further increases, the weakest bridge bonds in coal, such as ether bonds, thioether bonds, disulfides, aromatics, and fatty side chains, begin to break down and decompose. Oxygen-containing functional groups in coal will also be cracked, showing that fatty methyl groups are shed to form CH_4 and H_2, carbonyl groups are cracked to form CO, and the fatty bridge bond (-CH_2-CH_2-) is broken and sulfide (sulfur radical) is combined to form H_2S. The reaction can generate CH_4, C_2H_6, C_2H_4, and H_2O, CO, CO_2, and H_2S, and other gases, as shown in Figure 2 [13].

Table 1: Experimental sample parameter determination numerical value.

Industrial analysis (%)			Elemental analysis (%)				Sulfur composition (%)		
M_{ad}	A_d	V_{daf}	C	H	N	O	$S_{t,d}$	$S_{o,d}$	$S_{p,d}$
1.12	24.27	7.15	88.47	3.19	0.35	3.15	3.44	0.82	2.62

Hydrocarbon and nonhydrocarbon gaseous product changes are characterized in Figures 3–8. The generation of CH_4 is related to 5 aspects [14–16]: (1) adsorption of CH_4 in coal pores by thermal desorption, (2) fat side chain breakage on the coal surface, (3) pyrolysis of methylene bridge bonds in coal main structure, (4) pyrolysis of oxidized aromatic ring structure, and (5) broken fatty side chain in the aromatic structure. In the first stage, 250°C, the desorption of CH_4 adsorbed in coal pores happened. The second stage is 300~450°C, mainly formed by the breaking of aryl, alkyl, and ether bonds. The third stage 450/500~550°C, from relatively stable chemical bond cleavage, for example, the alkyl on the side chain of aromatic compounds breaks to form low molecular alkanes such as CH_4. After 550°C in the fourth stage, it was mainly the polycondensation between aromatic rings to form a condensed ring aromatic structure, which releases CH_4. With the addition of water and additives, the yield of methane and total gas is higher, which is expressed as "coal+water and $MgSO_4$ and $AlCl_3$" > "coal+water and $MgSO_4$" > "coal+water" > "coal." Comparison of the gas yield results showed that the presence of water and additives led to a significant increase in the total gas yield and methane gas yield, as shown in Figures 3 and 4.

Heavy hydrocarbons are dominated by C_2H_6, and their output increases first and then decreases as the temperature of the simulated experiment increases. Compared with the

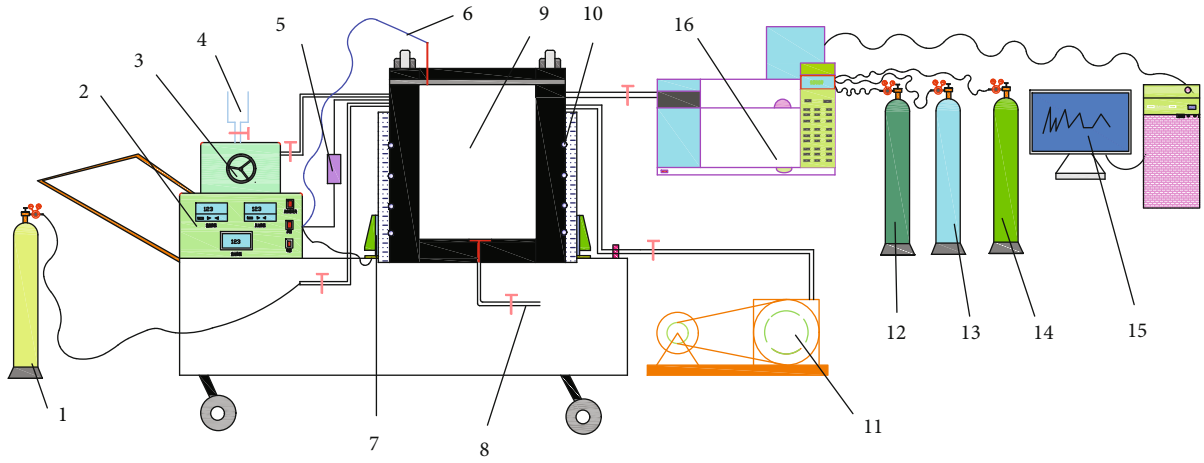

FIGURE 1: Schematic diagram of the experimental system. 1, 12, 13, 14—carrier gas cylinder; 2—controller; 3—pressure device; 4—liquid loading device; 5—pressure sensor; 6—temperature measuring device; 7—water circulation cooling device; 8—discharge port; 9—reactor body; 10—cooling circulation hole; 11—vacuum pump; 15—host; 16—chromatograph.

groups of "coal" and "coal+water," the addition of $MgSO_4$ makes the heavy hydrocarbon reach its maximum value at 400°C, which obviously reduces the temperature required to reach the peak of the heavy hydrocarbon yield and has a certain promotion effect on the formation of heavy hydrocarbon, as shown in Figure 5. Heavy hydrocarbons are mainly produced by the reaction of -OH attached to the C atom in the middle part of the aliphatic hydrocarbon chain in coal to form -COOH, and its formation can be described as follows [11]:

$$R - C(OH)_2 - CH_2 - CH_3 \longrightarrow R - COOH + C_2H_6 \quad (1)$$

$$R - CH_2 - C(OH)_2 - CH = CH_2 \longrightarrow R - CH_2 - COOH + C_2H_4 \quad (2)$$

$$R - CH_2 - C(OH)_2 - CH_2 - CH_2 - CH_3 \longrightarrow R - CH_2 - COOH + C_3H_8 \quad (3)$$

The heavy hydrocarbon yield decreases rapidly with increasing thermal simulation temperature after 400/450°C. The comparison revealed that the decrease in heavy hydrocarbon content was intensified in the presence of water, indicating that water was involved in the TSR reaction process, while the presence of additives accelerated the reaction of heavy hydrocarbons with sulfur-containing compounds and played a certain role in promoting it. The equation can be described as follows [11]:

$$C\left(\sum C_{n+1}H\right) + SO_4^{2-}(\text{Dissolved}) + H_2O \xrightarrow{Mg^{2+}/Al^{3+}} H_2S + CO_2 + HCO_3^- \quad (4)$$

The sources of H_2 were mainly polycondensation between free radicals and aromatic structures and polycondensation dehydrogenation reaction of hydrogenated aromatic structures [17–19]. The generation of H_2 in the first stage mainly includes hydrogen radicals mainly generated by the oxidation of hydrocarbons by minerals (sulfates) before 400°C, the cracking of long-chain aliphatic hydrocarbons to generate short-chain fatty radicals, and the secondary of light paraffins. Hydrogen radicals generated by cracking are combined with each other to generate hydrogen gas. At the second stage of 400~600°C, it is mainly formed by polycondensation between free radicals. They are the hydrogen radicals generated by the C-H bond breaking, cyclization, and aromatization of aliphatic hydrocarbons and the hydrogen radicals generated by the polycondensation reaction between aromatic rings and the reaction of C, CO, and H_2O. After 350°C, the H_2 yield drops significantly, and the H_2 formed by the C-H bond breakage reacts with sulfur radicals to generate H_2S. H_2 is generated only when there is a slight surplus, thereby reducing the hydrogen production rate. After the temperature reaches 500°C, it may be due to the insufficient supply of sulfur radicals in the sample and the deep reaction in the coal, such as the reaction of carbon and water and the reaction of CO and water to form H_2, which leads to an increase in the yield of H_2. In particular in the experimental conditions of anhydrous and water-free and salt-free addition of hydrogen, the hydrogen production has always been higher under the conditions of water-free and salt-free addition. This indicates that under anhydrous conditions, hydrogen consumption is lower and TSR is more difficult to occur, and water plays a very important role in TSR occurrence, which is consistent with the involvement of water in the TSR reaction mentioned earlier. The variation characteristics of H_2 production are shown in Figure 6, and its formation can be described as follows.

$$CO + H_2O \longrightarrow CO_2 + H_2 \quad (5)$$

$$C + 2H_2O \longrightarrow CO_2 + 2H_2 \quad (6)$$

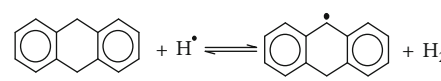

(7)

CO_2 is the hallmark product of TSR [12, 20, 21]. The precipitation of CO_2 between 250 and 350°C is mainly due to the

Table 2: Test results of gaseous products.

Media type	Temperature (°C)	CH_4 (mL/g)	$C_{2\sim5}$ (mL/g)	CO_2 (mL/g)	H_2 (mL/g)	H_2S (mL/g)
Coal	250	12.436	1.306	6.127	1.369	0.002
	300	13.758	1.432	7.264	1.410	0.006
	350	15.845	2.069	8.655	1.479	0.008
	400	18.828	2.845	9.655	1.319	0.013
	450	21.184	3.616	9.909	1.056	0.017
	500	22.621	3.855	10.073	0.871	0.016
	550	22.969	2.375	9.964	0.892	0.015
	600	23.128	0.986	9.627	1.012	0.009
Coal+deionized water	250	12.714	1.085	6.300	1.502	0.003
	300	14.941	1.416	8.182	1.519	0.008
	350	17.168	2.305	10.045	1.561	0.019
	400	20.625	3.077	10.545	1.641	0.035
	450	25.282	3.582	9.609	1.716	0.067
	500	27.247	2.537	9.991	1.748	0.072
	550	26.984	1.333	10.573	1.605	0.047
	600	26.387	0.393	10.095	1.487	0.023
Coal+deionized water+$MgSO_4$	250	13.288	1.143	6.380	1.430	0.004
	300	15.276	1.519	7.871	1.677	0.019
	350	17.722	2.645	10.468	1.704	0.062
	400	20.245	4.096	10.068	1.017	0.123
	450	27.157	2.984	9.151	0.530	0.165
	500	29.068	1.869	10.018	0.406	0.149
	550	29.456	1.016	10.287	0.419	0.102
	600	29.600	0.085	10.393	0.569	0.061
Coal+deionized water+$MgSO_4$+0.02 mol $AlCl_3$	250	13.765	1.109	6.585	1.372	0.004
	300	16.377	1.654	7.922	1.528	0.029
	350	19.066	3.281	9.467	1.597	0.099
	400	23.293	4.734	9.167	0.774	0.215
	450	30.099	3.811	8.806	0.417	0.276
	500	31.845	2.214	10.243	0.343	0.298
	550	32.132	0.842	10.815	0.364	0.230
	600	32.213	0.061	10.875	0.606	0.158

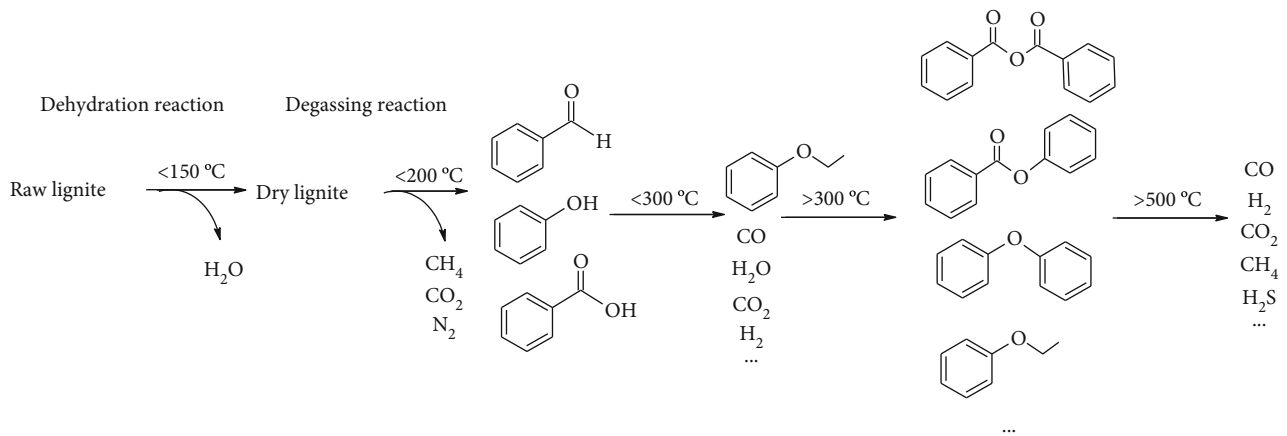

Figure 2: Reaction pathways for the briquette pyrolysis.

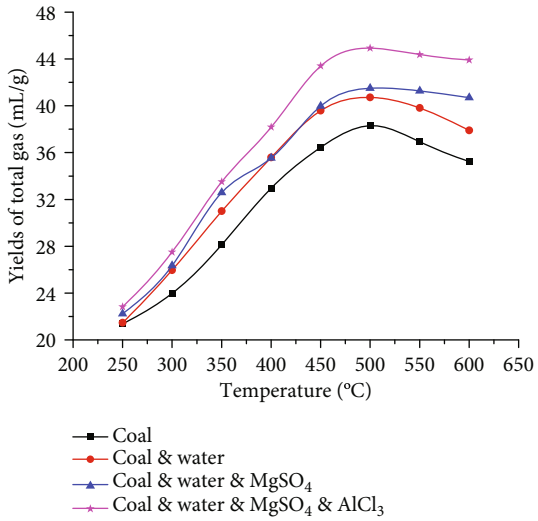

Figure 3: Variation characteristics of total gas.

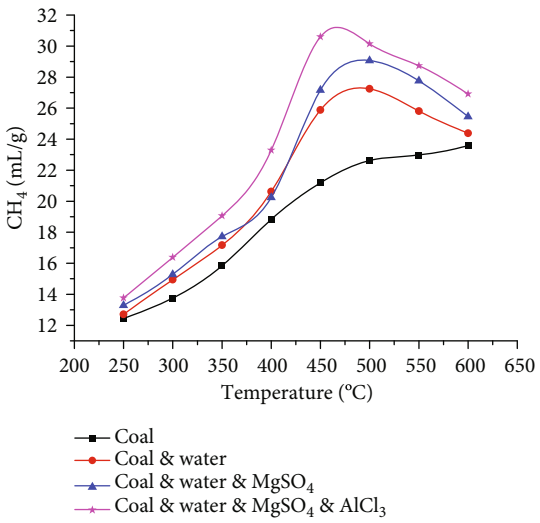

Figure 4: Variation characteristics of methane production.

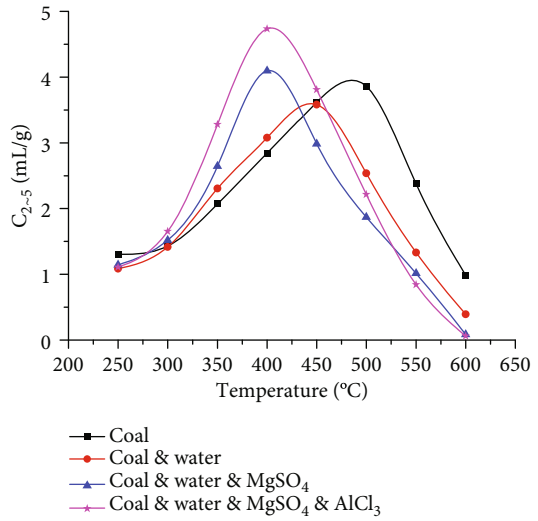

Figure 5: Variation characteristics of heavy hydrocarbon.

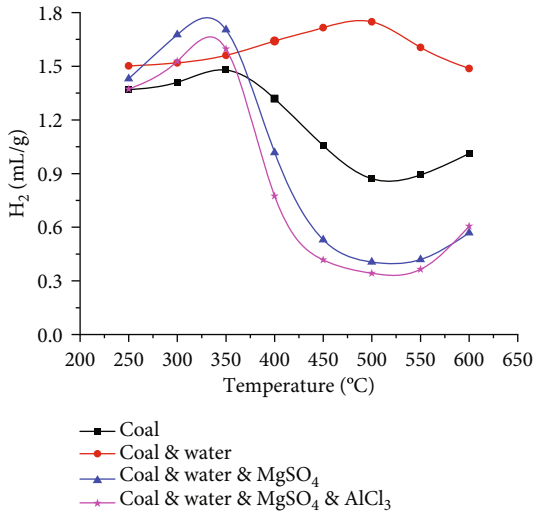

Figure 6: Variation characteristics of H_2 production.

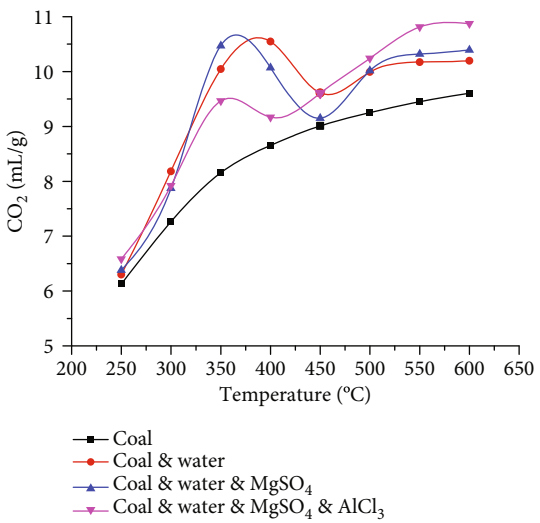

Figure 7: Variation characteristics of CO_2 production.

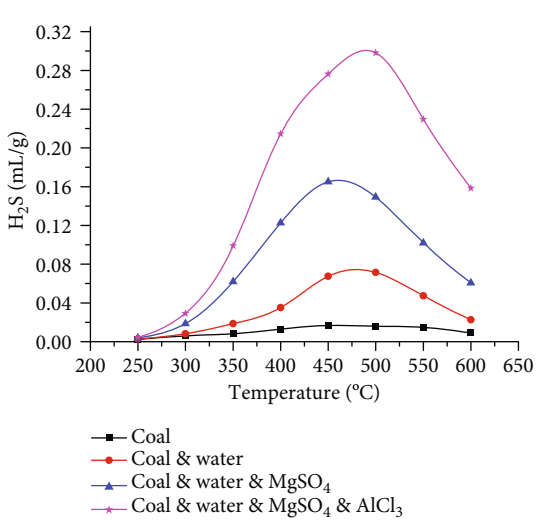

Figure 8: Variation characteristics of H_2S production.

decomposition of oxygen-containing carboxyl groups in coal by heat. After the temperature hits 350°C, most of the fatty bonds, oxygen-containing functional groups, and some aromatic weak bonds in coal are broken. Part of the broken carbonyl group is precipitated in the form of CO, and a part of it is combined with the oxygen atoms in the coal and precipitated in the form of CO_2. After the temperature reaches 450°C, the CO_2 precipitation gradually increases, indicating that deep TSR has occurred. From the four yield curves, it can be seen that the amount of CO_2 production is significantly increased with the participation of water compared with the "coal" group alone, while $MgSO_4$ and $AlCl_3$ have a certain driving effect on the TSR reaction. The variation characteristics of CO_2 production are shown in Figure 7.

Decomposition of carboxyl groups, ether bonds, and other oxygen-containing functional groups occurs [20]. The reaction occurs as follows:

$$\mathrm{R-COOH \longrightarrow RH + CO_2} \tag{8}$$

$$\mathrm{Ar-COOH + HOOC-Ar \longrightarrow Ar-O-Ar + H_2O + CO_2} \tag{9}$$

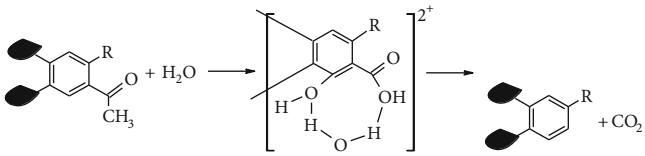

(10)

Sulfur in coal includes organic sulfur and inorganic sulfur. Most of the organic sulfur in coal is part of the molecular structure of kerogen, mainly including mercaptans, sulfides, disulfides, thiophenes, sulfoxides, and sulfones, and most of them are mainly thiophene sulfur [22–24]. Sulfur in coal includes organic and inorganic sulfur, and organic sulfur in coal is mostly a component of the molecular structure of cheese root, mainly including mercaptans, sulfides, disulfides, thiophene, sulfoxide, and sulfone and mainly thiophene sulfur [22–24]. Its shape is complex and diverse, and the thermal stability varies greatly. The precipitation, migration, and morphological distribution of sulfur during the TSR and pyrolysis process are affected by the pyrolysis environment and the kerogen structure and mineral species in coal. Inorganic sulfur usually exists in the form of sulfide, sulfate, and trace elemental sulfur, mainly pyrite [22, 25].

In the initial low-temperature stage, the TSR was low, and a small amount of H_2S may form by the bond breakage of unstable organic sulfur (such as thioether, thiol), hydrocarbon oxidation, and sulfate reduction. H_2S formed by hydrocarbon oxidation and sulfate reduction can in turn act as a catalyst to react with the dissolved form of sulfate to form S^0, so the production of H_2S was less. The possible reactions are as follows [8, 26, 27]:

$$\mathrm{HC + HSO_4^-(MgSO_4) \xrightarrow{Slow} \begin{bmatrix} SO_3 + HC \\ S_2O_3 \\ S^0 + HC \end{bmatrix} \begin{matrix} \xrightarrow{Rapid} H_2S + CO_2 + Tar \\ \xrightarrow{Rapid} SO_3 + S^0 \\ \xrightarrow{Rapid} H_2S + Tar \end{matrix}} \tag{11}$$

During thermal evolution, the formed hydrocarbons can react with the generated H_2S to produce organic sulfides.

$$\mathrm{H_2S + HC \longrightarrow \begin{bmatrix} R' - SH \\ R' - S_x - R' \end{bmatrix} \xrightarrow{\Delta} H_2S + R' - S^0 (R' \text{ is alkyl})} \tag{12}$$

As the temperature rises, unstable organic sulfides can undergo reduction reactions with sulfates.

$$\mathrm{\begin{bmatrix} R' - SH \\ R' - S_x - R' \end{bmatrix} + HSO_4^-(MgSO_4) \longrightarrow \begin{bmatrix} SO_3 + HC \\ S_2O_3 \\ S^0 + HC \end{bmatrix} \begin{matrix} \xrightarrow{Rapid} H_2S + CO_2 + Tar \\ \xrightarrow{Rapid} SO_3 + S^0 \\ \xrightarrow{Rapid} H_2S + Tar \end{matrix}} \tag{13}$$

The presence and formation of S^0 in turn provide a way for saturated hydrocarbons to be converted into naphthenic acids, aromatic hydrocarbons, and other sulfides, which usually contain two major blocks [28]:

The first block is dehydrogenation (oxidation):

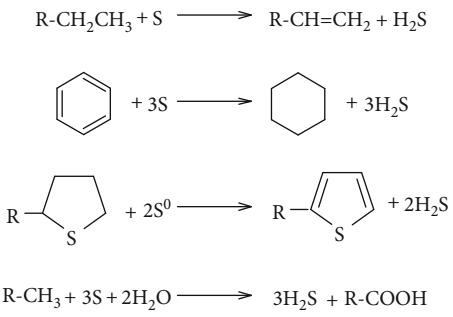

(14)

The second block is sulfide formation.

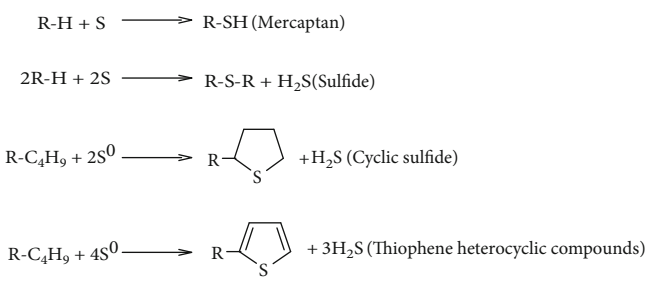

(15)

R is the fatty group.

Thiophene only begins to decompose at 450°C. The alkyl-substituted phosgene loses its alkyl group around 500°C, and the thiophene begins to decompose at 550°C. The thiophene

ring is stable, and decomposition begins only after at 800°C [29, 30]. The pyrolysis products of thiophene are usually some small-molecule compounds, such as sulfur, carbon, hydrogen sulfide, and acetylene. Under a hydrogen-rich atmosphere, these compounds react as follows [11, 31, 32]:

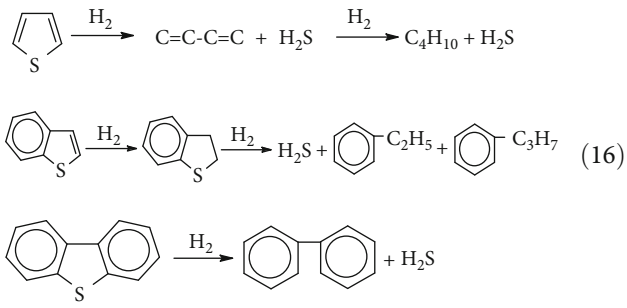

Thiophene compounds can be generated by the reaction of sulfur or H_2S with organic matter, or pyrite with organic molecules similar to ethylene, and salts such as bauxite and magnesium sulfate may promote the reaction.

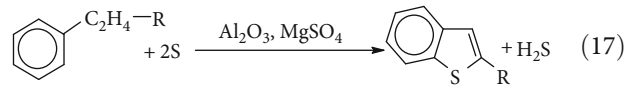

The sulfur in this experimental sample is mainly organic sulfur. The peak of H_2S precipitation reaches its maximum at 450~500°C, which obviously belongs to the form of sulfide. Subsequently, hydrogen sulfide is mainly formed by pyrite and thiophene sulfur, and FeS_2 can be reduced to FeS and H_2S at about 500°C. Structures such as aliphatic hydrocarbons and hydrogenated aromatic hydrocarbons in coal generate internal hydrogen radicals with hydrogen supply capability during the thermochemical reduction reaction, which promotes the reduction and decomposition of pyrite. The comparison of the hydrogen sulfide gas yield shows that the maximum yield of H_2S in the "coal+water and $MgSO_4$" system is 2.5 times higher than the maximum yield of H_2S in the "coal+water" system and 8.5 times higher than the maximum yield of H_2S in the "coal" system. This shows that the addition of $MgSO_4$ intensified the TSR reaction and promoted the production of H_2S gas. The variation characteristics of H_2S production are shown in Figure 8.

Water plays an important role as a solvent, reactant, and reaction carrier in aqueous thermal simulation reactions. The H element in the water is added to the coal sample under the synergistic effect of free radicals and ion effects, or ion exchange occurs with the minerals in the coal; it changes the environment of hydrothermal reaction to promote the cleavage of weak chemical bonds in the coal structure. In the process, it will also replace the oxygen-containing functional groups in the coal, so that the oxygen-containing functional groups decompose to form small-molecule gases and polar substances remaining in the water. It can also exchange with the hydrogen in coal and transfer in the coal structure. At the same time, the hydrogen and oxygen elements in the water may also be replaced by hydrogen atoms on the benzene ring under the synergistic effect of free radicals and ionic effects to form phenols.

4. Conclusion

The results of thermal simulation experiments showed that TSR promoted the cracking of coal, which led to an increase in the production of hydrogen sulfide and methane and a decrease in the production of heavy hydrocarbons. The presence of salts accelerates the evolution of hydrocarbon formation, and SO_4^{2-}, Al^{3+}, and Mg^{2+} contributed greatly to the TSR, resulting in an increase in the total amount of alkane gas and the production of H_2S and CO_2. Improving the salinity of the reaction system can promote the development of TSR.

In the thermal simulation system of coal, water is actually a hydrogen donor, providing some protonic hydrogen to stabilize the unstable intermediate material and accompanying the generation of H_2. In terms of gas production, the participation of water provides an additional source of hydrogen for the TSR reaction to produce gas, which accelerates the reaction and promotes gas production. Water media play an important role in the evolution of hydrocarbon generation.

Data Availability

The data used to support the findings of this study are available from the corresponding author upon request.

Conflicts of Interest

The authors declare that they have no conflicts of interest.

Acknowledgments

This work was supported by the National Natural Science Foundation of China under grant no. 51774116, the training plan of young backbone teachers in colleges and universities of Henan Province under grant no. 2019GGJS052, and the Fundamental Research Funds for the Universities of Henan Province under grant no. NSFRF200327.

References

[1] M. Liu, Q. Deng, and F. Zhao, "Origin of hydrogen sulfide in coal seams in China," *Safety Science*, vol. 50, no. 4, pp. 1031–1038, 2012.

[2] H. G. Machel, "Bacterial and thermochemical sulfate reduction in diagenetic settings – old and new insights," *Sedimentary Geology*, vol. 140, no. 1-2, pp. 143–175, 2001.

[3] M. M. Cross, D. A. C. Manning, S. H. Bottrell, and R. H. Worden, "Thermochemical sulphate reduction (TSR): experimental determination of reaction kinetics and implications of the observed reaction rates for petroleum reservoirs," *Organic Geochemistry*, vol. 35, no. 4, pp. 393–404, 2004.

[4] X. Wang, Q. Ma, H. Chaojie, and R. Lin, "Study on formation mechanism of H_2S by thermochemical sulfate reduction of thiolane and magnesium sulphate," *Journal of China University of Petroleum (Edition of Natural Science)*, vol. 44, no. 1, pp. 156–162, 2020.

[5] R. H. Worden, W. J. Carrigan, and P. J. Jones, "Origin of H_2S in Khuff reservoirs by thermochemical sulfate reduction: evidence from fluid inclusions," *Saudi Aramco Journal of Technology*, vol. 1, pp. 42–52, 2004.

[6] K. Ding, S. Li, C. Yue, and N.-N. Zhong, "Simulation experiments on thermochemical sulfate reduction using natural gas," *Journal of Fuel Chemistry & Technology*, vol. 35, no. 4, pp. 401–406, 2007.

[7] C. Cai, Y. Tang, K. Li, K. Jiang, C. Jiang, and Q. Xiao, "Relative reactivity of saturated hydrocarbons during thermochemical sulfate reduction," *Fuel*, vol. 253, pp. 106–113, 2019.

[8] T. Zhang, G. S. Ellis, C. C. Walters, S. R. Kelemen, K.-s. Wang, and Y. Tang, "Geochemical signatures of thermochemical sulfate reduction in controlled hydrous pyrolysis experiments," *Organic Geochemistry*, vol. 39, no. 3, pp. 308–328, 2008.

[9] S. Zhang, H. Huang, J. Su, M. Liu, X. Wang, and J. Hu, "Geochemistry of Paleozoic marine petroleum from the Tarim Basin, NW China: part 5. Effect of maturation, TSR and mixing on the occurrence and distribution of alkyldibenzothiophenes," *Organic Geochemistry*, vol. 86, pp. 5–18, 2015.

[10] B. C. Biehl, L. Reuning, J. Schoenherr, V. Lüders, and P. A. Kulka, "Impacts of hydrothermal dolomitization and thermochemical sulfate reduction on secondary porosity creation in deeply buried carbonates: a case study from the Lower Saxony Basin, Northwest Germany," *American Association of Petroleum Geologists Bulletin*, vol. 100, no. 4, pp. 597–621, 2016.

[11] Q. Deng, J. Yin, T. Zhang, and H. Wang, "Gas-producing characteristics of coals containing hydrogen sulfide by the thermochemical sulfate reduction," *Thermal Science*, vol. 24, no. 4, pp. 2475–2483, 2020.

[12] W. Liu and X. Yongchang, "A two-stage model of carbon isotopic fractionation in coal-gas," *Geochimica*, vol. 4, pp. 359–366, 1999.

[13] S. Cui and W. Lv, "Effect of polyvinyl alcohol on pyrolysis of briquette," *Journal of Sichuan University (Natural Science Edition)*, vol. 54, no. 6, pp. 1269–1274, 2017.

[14] Q. Deng, X. Wu, and Y. Wang, "Experimental study on thermochemical sulfate reduction reaction with coal," *Coal Conversion*, vol. 42, no. 6, pp. 70–76, 2019.

[15] Q. Xiao, A. Amrani, Y. Sun et al., "The effects of selected minerals on laboratory simulated thermochemical sulfate reduction," *Organic Geochemistry*, vol. 122, pp. 41–51, 2018.

[16] K. Li, S. C. George, C. Cai et al., "Fluid inclusion and stable isotopic studies of thermochemical sulfate reduction: Upper Permian and Lower Triassic gasfields, northeast Sichuan Basin, China," *Geochimica et Cosmochimica Acta*, vol. 246, pp. 86–108, 2019.

[17] G. S. Ellis, W. Said-Ahmad, P. G. Lillis, L. Shawar, and A. Amrani, "Effects of thermal maturation and thermochemical sulfate reduction on compound-specific sulfur isotopic compositions of organosulfur compounds in Phosphoria oils from the Bighorn Basin, USA," *Organic Geochemistry*, vol. 103, pp. 63–78, 2017.

[18] M. Sośnicka and V. Lüders, "Fluid inclusion evidence for low-temperature thermochemical sulfate reduction (TSR) of dry coal gas in Upper Permian carbonate reservoirs (Zechstein, Ca2) in the North German Basin," *Chemical Geology*, vol. 534, no. 20, p. 119453, 2020.

[19] M. A. Alrowaie, A. M. Jubb, A. Schimmelmann, M. Mastalerz, and L. M. Pratt, "Hydrous heating experiments at 130°C yield insights into the occurrence of hydrogen sulfide and light alkanes in natural gas reservoirs," *Organic Geochemistry*, vol. 137, p. 103901, 2019.

[20] S. Yuan, G. S. Ellis, I. M. Chou, and R. C. Burruss, "Experimental investigation on thermochemical sulfate reduction in the presence of 1-pentanethiol at 200 and 250°C: implications for in situ TSR processes occurring in some MVT deposits," *Ore Geology Reviews*, vol. 91, pp. 57–65, 2017.

[21] D. Morad, F. H. Nader, S. Morad et al., "Limited thermochemical sulfate reduction in hot, anhydritic, sour gas carbonate reservoirs: the Upper Jurassic Arab Formation, United Arab Emirates," *Marine and Petroleum Geology*, vol. 106, pp. 30–41, 2019.

[22] W. Li, Y. Tang, Q. Zhao, and Q. Wei, "Sulfur and nitrogen in the high-sulfur coals of the Late Paleozoic from China," *Fuel*, vol. 155, pp. 115–121, 2015.

[23] C. Chen-Lin, "Sulfur in coals: a review of geochemistry and origins," *International Journal of Coal Geology*, vol. 100, pp. 1–13, 2012.

[24] L. Gonsalvesh, S. P. Marinov, M. Stefanova, R. Carleer, and J. Yperman, "Organic sulphur alterations in biodesulphurized low rank coals," *Fuel*, vol. 97, pp. 489–503, 2012.

[25] S. Phillips, R. M. Bustin, and L. E. Lowe, "Earthquake-induced flooding of a tropical coastal peat swamp: a modern analogue for high-sulfur coals?," *Geology*, vol. 22, no. 10, pp. 929–932, 1994.

[26] P. Pirzadeh, S. Raval, and R. A. Marriott, "On the fate of hydraulic fracturing fluid additives: thermochemical sulfate reduction reaction of sodium dodecyl sulfate," *Organic Geochemistry*, vol. 83-84, pp. 94–100, 2015.

[27] G. Zhu, Y. Zhang, Z. Zhang et al., "High abundance of alkylated diamondoids, thiadiamondoids and thioaromatics in recently discovered sulfur-rich LS2 condensate in the Tarim Basin," *Organic Geochemistry*, vol. 123, pp. 136–143, 2018.

[28] B. Zheng, G. Ten, J. Zhang, G. Renxiang, and L. Wenhui, "Origin of H_2S from TSR and TDR reactions in oil/gas reservoirs in the Feixianguan Formation the northeastern Sichuan Basin," *Oil & Gas Geology*, vol. 31, no. 6, pp. 847–856, 2010.

[29] O. H. Ardakani, A. Chappaz, H. Sanei, and B. Mayer, "Effect of thermal maturity on remobilization of molybdenum in black shales," *Earth and Planetary Science Letters*, vol. 449, pp. 311–320, 2016.

[30] C. Yue, S. Li, and H. Song, "Impact of TSR experimental simulation using two crude oils on the formation of sulfur compounds," *Journal of Analytical and Applied Pyrolysis*, vol. 109, pp. 304–310, 2014.

[31] J. Aali and O. Rahmani, "H_2S–origin in South Pars gas field from Persian Gulf, Iran," *Journal of Petroleum Science and Engineering*, vol. 86-87, pp. 217–224, 2012.

[32] P. Mougin, V. Lamoureux-Var, A. Bariteau, and A. Y. Huc, "Thermodynamic of thermochemical sulphate reduction," *Journal of Petroleum Science & Engineering*, vol. 58, no. 3-4, pp. 413–427, 2007.